microbial biotechnology

Open Access

E. coli biofilm formation and its susceptibility towards T4 bacteriophages studied in a continuously operating mixing – tubular bioreactor system

Ana Lisac[1] Elfi Birsa[1] and Aleš Podgornik[1,2]*

[1]*Faculty of Chemistry and Chemical Technology, University of Ljubljana, Večna pot, 113, Ljubljana, Slovenia.*

[2]*COBIK, Mirce 21, 5270, Ajdovščina, Slovenia*

.

Summary

A system consisting of a connected mixed and tubular bioreactor was designed to study bacterial biofilm formation and the effect of its exposure to bacteriophages under different experimental conditions. The bacterial biofilm inside silicone tubular bioreactor was formed during the continuous pumping of bacterial cells at a constant physiological state for 2 h and subsequent washing with a buffer for 24 h. Monitoring bacterial and bacteriophage concentration along the tubular bioreactor was performed via a piercing method. The presence of biofilm and planktonic cells was demonstrated by combining the piercing method, measurement of planktonic cell concentration at the tubular bioreactor outlet, and optical microscopy. The planktonic cell formation rate was found to be 8.95×10^{-3} h^{-1} and increased approximately four-fold (4×) after biofilm exposure to an LB medium. Exposure of bacterial biofilm to bacteriophages in the LB medium resulted in a rapid decrease of biofilm and planktonic cell concentration, to below the detection limit within < 2 h. When bacteriophages were supplied in the buffer, only a moderate decrease in the concentration of both bacterial cell types was observed. After biofilm washing with buffer to remove unadsorbed bacteriophages, its exposure to the LB medium (without bacteriophages) resulted in a rapid decrease in bacterial concentration: again below the detection limit in < 2 h.

Received 2 February, 2022; accepted 10 May, 2022.
*For correspondence. E-mail ales.podgornik@fkkt.uni-lj.si; Tel. +386 (0)1 479 8584.
Microbial Biotechnology (2022) **15**(9), 2450–2463.

doi:10.1111/1751-7915.14079

Funding Information

The financial support is gratefully acknowledged from the Slovenian Research Agency (ARRS) through programme P1-0153 and project J7-2603 as well as from project IMBI co-financed by European Regional Development Fund, Interreg V-A Italy-Slovenia programme 2014-2020.

Introduction

Bacterial biofilms are dynamic structures of bacteria (Costerton *et al.*, 1999; Azeredo *et al.*, 2021) that develop on inert surfaces, such as medical implants and medical devices (Donlan, 2001, 2002), dead and living tissues (Lambe *et al.*, 1991; Costerton *et al.*, 1999), and pose a serious global threat due to their tolerance to host immune defences and antibiotic treatments (Marrie *et al.*, 1982; Costerton *et al.*, 1999; Hall-Stoodley *et al.*, 2004; De la Fuente-Núñez *et al.*, 2013; Sharma *et al.*, 2019). These structures are clusters formed by single (Tolker-Nielsen *et al.*, 2000; Su *et al.*, 2012) or multiple bacterial species (Burmølle *et al.*, 2006) that are generally less metabolically active and therefore less affected by antibiotics (Davies, 2003; Stewart, 2015; Sønderholm *et al.*, 2017). Bacteria are connected within a biofilm matrix consisting of extracellular polymeric substances (EPS), such as exopolysaccharides, extracellular DNA, and proteins (Zhang *et al.*, 1998; Sutherland *et al.*, 2004; Flemming *et al.*, 2007; Flemming and Wingender, 2010), which are produced by the bacteria in response to the absence of a substrate in the environment and serve as a physical barrier.

Biofilms play a significant role in persistent inflammation (Costerton *et al.*, 2003; Jamal *et al.*, 2018; Svensson Malchau *et al.*, 2021) and antibiotic tolerance, (Sharma *et al.*, 2019) as they are formed to protect bacteria and grant survival of a community in an inhospitable environment. Biofilm formation begins with the adsorption of free-floating bacteria to a surface and continues with bacterial adhesion (Davies *et al.*, 1993; Davies and Geesey, 1995; Tuson and Weibel, 2014). Due to adverse conditions and stress signals, biofilm development must be rapid to prevent the death of the bacterial population. The expression of genes to stimulate the biosynthesis of adhesion and EPS components occurs; (Whiteley *et al.*, 2001; Beloin and Ghigo, 2005) once strong adhesion is attained, bacteria begin to grow, divide, accumulate, and form an EPS matrix for structural support and protection (Keleştemur *et al.*, 2018).

The composition of the EPS matrix varies from biofilm to biofilm but typically accounts for approximately 50–90% of the biofilm (Flemming and Wingender, 2010; Dhayakaran and Neethirajan, 2017; Jamal *et al*., 2018). With EPS production and bacterial growth, the biofilm begins to mature and thicken, generating multiple layer structures that differ between environmental conditions and bacterial species (O'Toole and Kolter, 1998; Vu *et al*., 2009). Once a biofilm has developed, the detachment of biofilm parts due to shear or mechanical stress, or bacteria-regulated multiplication and dispersion of planktonic bacteria occurs to continue the colonization of new surfaces (Stoodley *et al*., 2001; Sauer *et al*., 2002; Hall-Stoodley *et al*., 2004; De la Fuente-Núñez *et al*., 2013).

Mature biofilms cause a range of chronic infections, since their eradication is extremely difficult (Lewis, 2001). Biofilms are also a source of planktonic bacteria that can cause acute infections and are susceptible to antibiotic therapy. New planktonic bacteria can be released from biofilms constantly, causing a recurrence of symptoms (Read *et al*., 1989; Costerton *et al*., 1999, 2003).

To avoid several antibiotic treatments and the possibility of antibiotic resistance, new, efficient anti-biofilm therapies are needed. Bacteriophages ('phages' for short) represent suitable anti-biofilm agents (Doolittle *et al*., 1995; Alves *et al*., 2016; Forti *et al*., 2018; Hansen *et al*., 2019). Lytic phages are viruses that use bacteria for their propagation and kill them (Ackermann and Prangishvili, 2012). In terms of biofilm removal, phages show interesting properties as they produce enzymes that facilitate their penetration into bacterial biofilm and eventually its disruption (Hughes *et al*., 1998a,b; Abedon, 2015; Simmons *et al*., 2018). Besides, they are specific, allow automatic dosing at the infection site, and avoid the occurrence of side effects when used for therapeutic purposes. However, in order to use phages as therapeutic anti-biofilm agents, it is necessary to understand their adsorption, infection, propagation, and lysis, to optimally exploit their potential for biofilm eradication. This is of significant importance since the efficacy of phages against bacterial biofilms depends on the biofilm structure (Sutherland *et al*., 2004).

To investigate phage efficacy against bacterial biofilms under controlled conditions, a continuously operating system consisting of a mixing bioreactor, operating like a chemostat, and a tubular bioreactor, connected in series was developed. Proof of principle was demonstrated using phage T4 and bacteria host *Escherichia coli* as a model system. The bacterial biofilm was formed on the inner wall of the tubular silicone bioreactor under defined conditions, at a constant temperature, linear velocity, and bacterial physiological state during supply, determined by chemostat dilution rate. This set-up enabled studying the properties of the bacterial biofilm and its eradication when exposed to phages in the presence of substrate or under substrate limitation.

Results and discussion

Experimental set-up

The experimental set-up shown in Fig. 1A was developed to investigate the formation of *E. coli* bacteria biofilm and its eradication using phages. It consisted of a chemostat, providing the flow of bacteria in a constant physiological state, SM buffer flow, and a silicone tubular bioreactor mimicking in particular case silicone urinary catether (Read *et al*., 1989; Stickler, 1996; Donlan, 2001; Koseoglu *et al*., 2006; Wilks *et al*., 2021) inside which a biofilm can be formed. The sampling of bacteria along the tubular bioreactor was performed by the piercing method, which consisted of several steps (Fig. 1B). First, a thin, sterile syringe needle was used to pierce the bioreactor wall at various positions. Due to the small needle diameter (OD 0.35 mm), the elastic silicone tubing spontaneously sealed after the needle was removed, preventing contamination. When the needle penetrated the silicone tubing entering into a tubular bioreactor (Fig. 1B), it was assumed that a small portion of the biofilm was cut and remained in the needle. Once the needle was inside the bioreactor, an additional 50 µl of the medium was collected, potentially containing free-floating bacteria. In this way, both types of bacteria could be sampled simultaneously together with unadsorbed phages (when present). Set-up enabled studying biofilm formation and the effect of its exposure to phages, according to the design of the experiments presented in Fig. 1C.

Biofilm formation

To form a bacterial biofilm, *E. coli* bacteria in LB medium from the chemostat were continuously mixed with SM buffer (1:1 ratio – Fig. 1A) and allowed to adhere to the inner surfaces of the tubular bioreactor. With the LB medium, an essential concentration of nutrients for the formation and growth of bacterial clusters on the walls was provided, initiating biofilm growth and EPS production (Guzmán-Soto *et al*., 2021), while the SM buffer was used to enhance growth-limiting conditions. Bacteria were supplied into the tubular bioreactor for 2 h at a flow rate of 0.2 ml min^{-1}, corresponding to a linear velocity of 0.01 m min^{-1}, providing laminar flow conditions.

During the bacterial supply, samples were taken from different positions of the tubular bioreactor by the piercing method, representing different residence times $\tau(t)$ of the bacteria inside the bioreactor. The bacterial

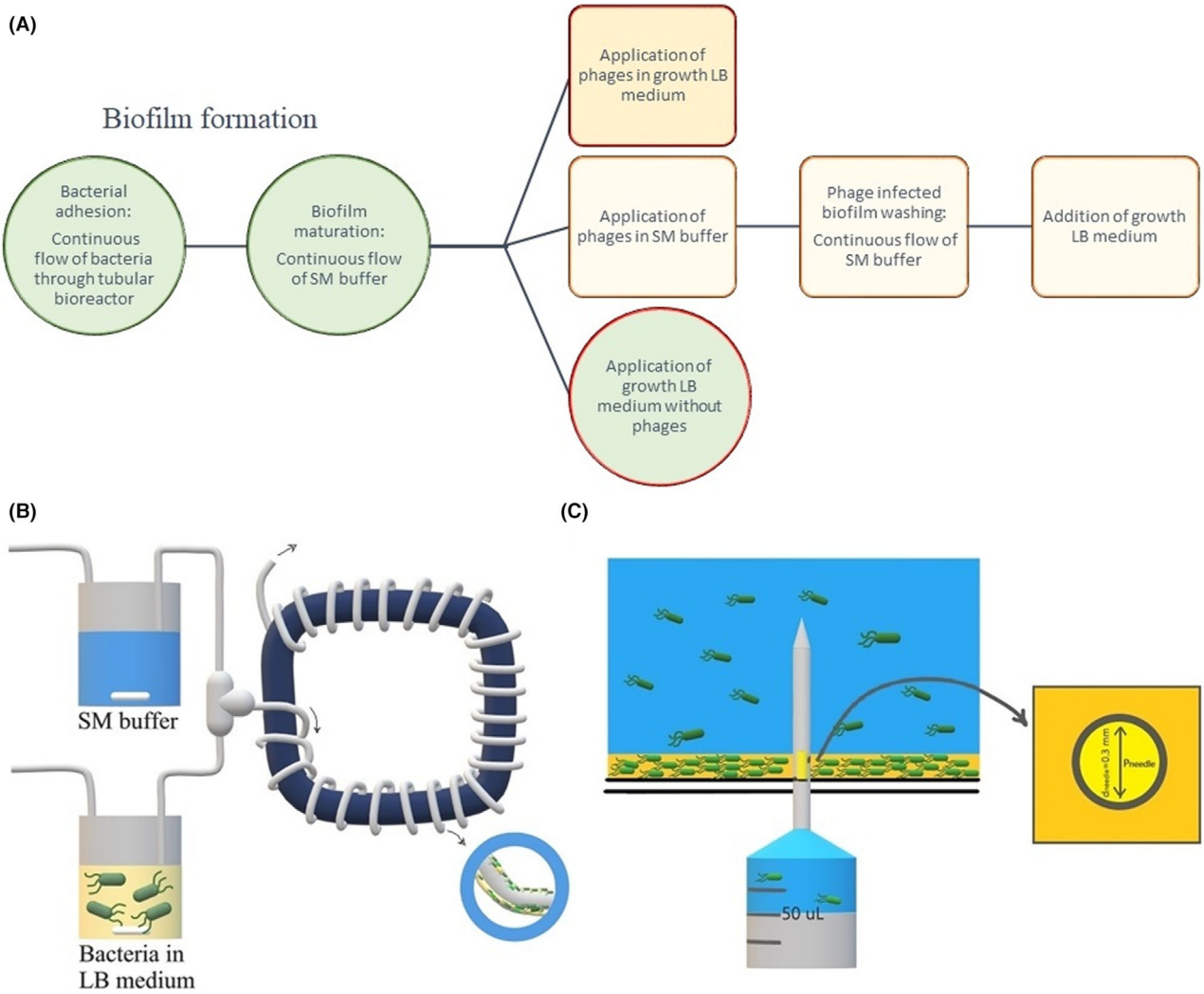

Fig. 1. A set-up of continuous bioreactor system (A), schematic diagram of piercing sampling method (B), and flowchart of experiments (C).
A. Experiments were performed in a chemostat system connected to a tubular bioreactor – a silicone tube within which biofilm was formed.
B. Sampling along tubular bioreactor was performed by a piercing method using a sterile syringe needle, where small biofilm sample was collected during piercing and taken in with 50 μl of medium additionally collected from the tubular bioreactor. The sampled area of bacterial biofilm was defined by needle size.
C. All experiments started with the formation of a steady-state biofilm, which was investigated under substrate limitation and optimal growth conditions. Phages were applied to the biofilm in both, the substrate limiting and growth medium, and their effect was studied.

concentration determined 1 h after the start of continuous bacteria supply, shown in Fig. S1, demonstrates that almost constant bacterial concentration along the tubular bioreactor was present. This indicated that cell adsorption on the inner wall was slow (if present at all), as no constant decrease in concentration along the bioreactor was observed. Constant bacterial concentration is expected to result in the formation of a uniform bacterial biofilm throughout the tubular bioreactor.

After 2 h of continuous bacteria supply in diluted medium, the bacterial flow was stopped and replaced by solely SM buffer flow to remove unadsorbed bacteria, limit nutrient supply and therefore promoting biofilm formation on the inner wall of the tubular bioreactor (Flemming *et al.*, 2007; Sharma *et al.*, 2019). Washing with SM buffer continued for 24 h, allowing biofilm maturation. Bacterial biofilms also generate planktonic bacteria (Ward *et al.*, 1992; Costerton *et al.*, 1999, 2003; Mah and O'Toole, 2001; Hall-Stoodley *et al.*, 2004; Bjarnsholt, 2013) that spread potential bacterial infections (Sharma *et al.*, 2016) and cause acute infections (Bjarnsholt, 2013). Because of that, it is important to monitor both, concentration of biofilm and planktonic bacteria. Total bacterial concentration during washing was monitored by the piercing method at various residence times along the bioreactor (Fig. 2A).

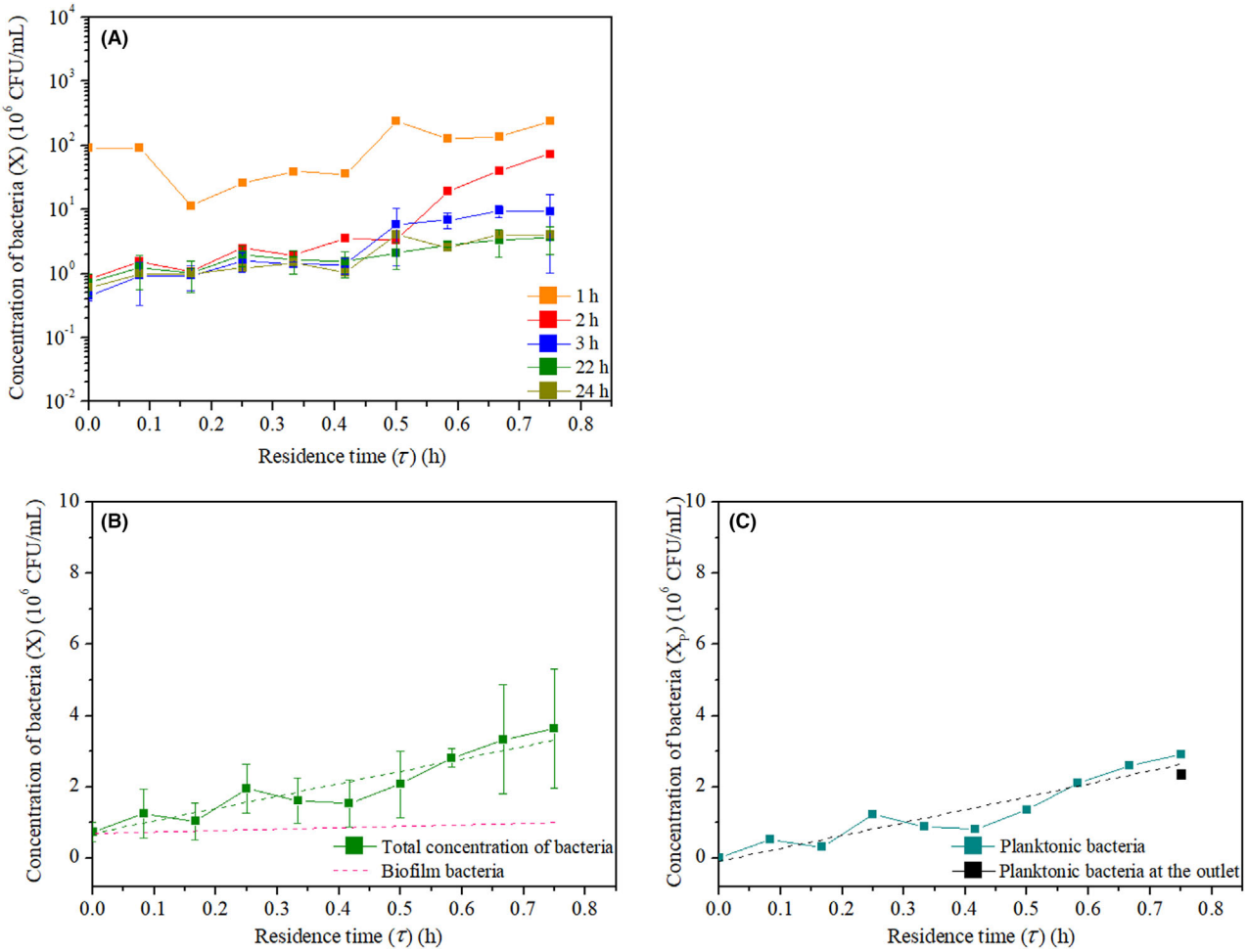

Fig. 2. Concentration of bacteria in the tubular bioreactor during biofilm washing with SM buffer (A), total concentration of bacteria, concentration of total and estimated biofilm (B), and estimated planktonic bacteria (C) inside the tubular bioreactor after 24 h of washing the biofilm with SM buffer.

A. SM buffer was continuously supplied to the tubular bioreactor to wash unadsorbed bacteria. The concentration of bacteria was monitored at different positions of the tubular bioreactor (representing different residence times) for several hours until reaching constant bacterial concentration.

B. Green squares with error bars represent the experimental data of total bacteria concentration, the dashed green line represents its linear fit, while the dashed pink line represents the estimated concentration of bacteria in the biofilm.

C. The concentration values of planktonic bacteria, which is the difference between measured total bacteria concentration and estimated biofilm concentration, are represented by blue squares, while the black dashed line represents its linear fit, and black square represents the concentration of planktonic bacteria at the outlet of the bioreactor.

The data, based on the analysis of three independent experiments, showed that the bacterial concentration in the tubular bioreactor decreased until a steady state was reached somewhere between the 3 and 22 h. As no new bacteria were introduced into the tubular bioreactor during washing, detected bacteria should represent potential biofilm (X_B) and/or planktonic (X_P) bacteria. To discriminate between the two types, the bacterial concentration at the bioreactor outlet ($X_{P\ outlet}$) was determined by collecting the outlet medium after 24 h of washing, containing therefore only free-floating planktonic bacteria. Their concentration was determined to be 2.63×10^6 CFU ml^{-1}. Subtracting this value from the total bacterial concentration determined by the piercing method at the bioreactor end ($\tau = 0.75$ h) resulted in a concentration of 9.97×10^5 CFU ml^{-1}, representing biofilm bacteria (X_B). Interestingly, this value is similar to the total bacterial concentration obtained by the piercing method at the beginning of the bioreactor ($\tau = 0$ h), namely $(0.73 \pm 0.28) \times 10^6$ CFU ml^{-1}. Since no free bacterial cells enter the tubular bioreactor, the total bacteria concentration at $\tau = 0$ h should therefore represent concentration of biofilm bacteria (X_{B0}). The similar concentration of biofilm bacteria at the beginning and end of

the tubular bioreactor confirmed that a uniform biofilm has formed throughout the tubular bioreactor, as could be anticipated from a constant bacteria concentration along the bioreactor during their supply (Fig. S1). This conclusion is also supported by microscopic images of biofilm from different positions (Fig. S2). Uniform biofilm also explains the linear increase in total bacteria concentration along the tubular bioreactor (Fig. 2B). If planktonic cells are formed by bacteria biofilm uniformly, their generation throughout the bioreactor is constant what results in the observed trend.

To investigate whether the bacteria detected at the outlet of the tubular bioreactor were planktonic bacteria or detached biofilm aggregates, the bacterial sample was examined with an optical microscope. Only single floating cells without aggregates were observed (data not shown). This could be anticipated due to a constant, laminar flow regime within the bioreactor (Reynolds number = 0.51) causing a shear rate of only 17.06 s^{-1} and shear stress of only 0.026 Pa on the bacterial biofilm; therefore, no biofilm disruption is expected. To investigate the morphology of the biofilm on the inner silicone wall, optical microscopy was again applied (Fig. 3 A and B).

The images show the biofilm presence on the inner part of the silicone wall that was of non-uniform thickness. Nevertheless, to simplify its description, the average thickness was determined from the images and found to be around 13 μm. Doing so enabled the estimation of cell packing within the biofilm. *E.coli* bacteria are rod-shaped (Reshes *et al.*, 2008) with an approximate size of $1 \times 1 \times 2$ μm and a volume of 2 μm^3 (Riley, 1999). Bacteria were sampled from an area corresponding to the cross-section of the inlet needle ($P_{syringe\ needle} = 7.06858 \times 10^{-8}$ m^2), and the average content of sampled bacteria was 3.45×10^4 CFU (6.91×10^5 CFU $ml^{-1} \times 50$ μl). In the case of tight bacteria packing within the biofilm, 7.07×10^{-2} mm^2 of the biofilm with an estimated thickness of 13 μm would contain 4.59×10^5 bacteria. The ratio between the measured bacteria in the biofilm and maximal bacteria number at tight packing represents the volumetric fraction occupied by bacterial cells in the actual biofilm. The obtained value of 7.52% fits within the range of values observed in bacterial biofilms (Corbin *et al.*, 2001; McLean *et al.*, 2001; Flemming and Wingender, 2010).

Based on the demonstrated presence of the biofilm, it seems reasonable to conclude that the planktonic cells are generated by biofilm bacteria. Therefore, it would be worthwhile to estimate their dispersion rate. This parameter can be calculated by dividing the amount of planktonic bacteria exiting the tubular bioreactor by the amount of biofilm bacteria.

The total amount of biofilm bacteria can be estimated from the amount of bacteria sampled by the piercing method at the $\tau = 0$ h of the tubular bioreactor (3.45×10^4 CFU on the area of $P_{syringe\ needle} = 7.06858 \times 10^{-8}$ m^2), extrapolating it to the total inner wall area. Considering that uniform biofilm is present and the total inner surface area of the tubular bioreactor (Fig. 1B) is 7.226×10^{-3} m^2, one can calculate the total amount of biofilm bacteria in the bioreactor to be 3.53×10^9. Since the concentration of planktonic bacteria exiting the tubular bioreactor was 2.63×10^6 CFU ml^{-1} (Fig. 2C) at a flow rate of 0.2 ml min^{-1}, approximately 5.27×10^5 planktonic cells have been generated every minute (3.16×10^7 CFU h^{-1}). The ratio between the planktonic bacteria formation rate and total biofilm bacteria provides an average planktonic cells generation rate of

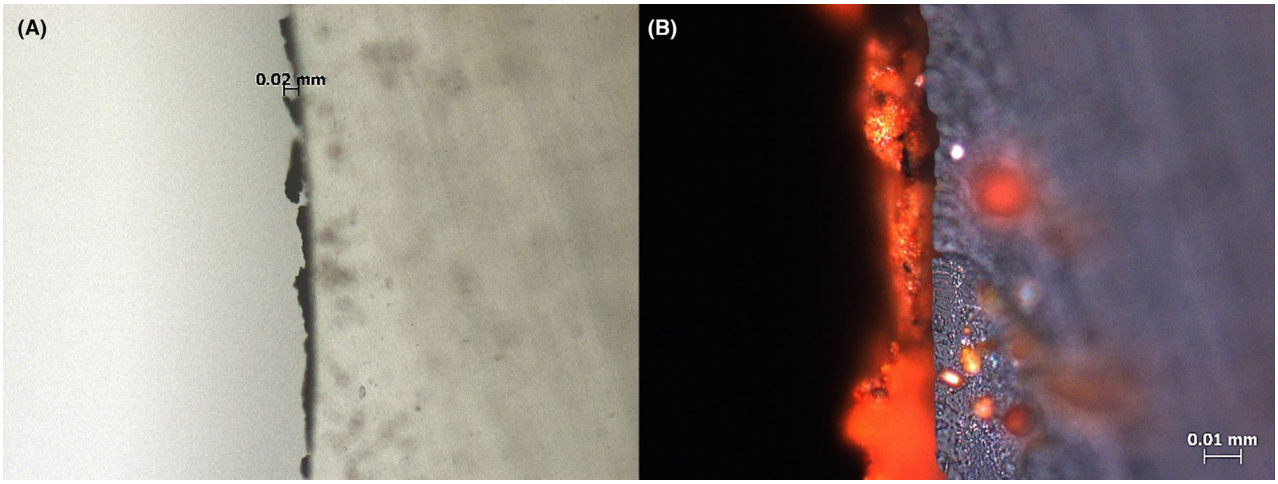

Fig. 3. Image of bacterial biofilm after 24 h of continuous SM buffer flow through the tubular bioreactor on optical microscope (A) under transmitted and (B) under reflected light.

8.95×10^{-3} h^{-1}. On the other hand, constant bacterial biofilm concentration between 22 and 24 h of SM buffer washing (Fig. 2A) indicated that all bacterial cells formed by the biofilm were released into the medium as planktonic bacteria.

Effect of LB medium on formed biofilm

To investigate the viability of formed bacterial biofilm, the LB medium flow was introduced into a tubular bioreactor, and the bacterial concentration was monitored by the piercing method (Fig. 4).

A significant increase in bacterial concentration along the bioreactor can be observed after substrate addition, indicating faster generation of planktonic bacterial cells. In addition, the higher bacterial concentration at the entrance of the bioreactor ($\tau = 0$ h) also indicated an increase in bacterial biofilm concentration after the addition of fresh nutrients (Fig. 4).

To estimate the generation rate of bacteria inside the tubular bioreactor after substrate addition, we can presume that the bacterial concentration at $\tau = 0$ h represents the biofilm bacteria (1.366×10^7 CFU ml^{-1}). Therefore, the concentration of planktonic bacteria along the bioreactor can be calculated by subtracting the biofilm cells from the total bacteria concentration at $\tau = 0.75$ h (1.91×10^8 CFU ml^{-1}), again assuming that the biofilm is uniform along the bioreactor. The number of biofilm bacteria inside the tubular bioreactor after LB addition is 6.98×10^{10}. Since 3.82×10^7 planktonic bacteria were generated every minute, their formation rate increased to 0.0328 h^{-1} after LB addition, which is almost 4-fold higher compared to the substrate limitation conditions.

Phage interaction with bacterial biofilm

Application of phages in LB medium. Phages, as bacterial viruses, have interesting properties in terms of biofilm control and elimination, as they can invade and affect the structure of biofilms (Abedon, 2011), multiply at the site of infection, and lyse bacteria. Phage multiplication is greatly affected by the physiological state of planktonic bacteria (Hadas *et al.*, 1994, 1997; Abedon *et al.*, 2001; Golec *et al.*, 2014; Nabergoj *et al.*, 2018b). Phages replicate more effectively in bacterial cells cultivated under optimal growth conditions, whereas they have little or no effect in bacteria with reduced metabolism and low specific growth rate (Abedon *et al.*, 2001; Łoś and Wegrzyn, 2012; Cenens *et al.*, 2013). One can speculate that this phenomenon would play an important role also for biofilms where bacteria of different physiological state are present (Sternberg *et al.*, 1999) and affected by nutrients (Stoodley *et al.*, 1999).

To investigate phage adsorption, infection of the biofilm and phage propagation, the formed biofilm was exposed to phages by pumping them through the tubular bioreactor in LB medium, which provided the necessary nutrients for the biofilm bacteria. Phage and bacteria concentrations were monitored along the bioreactor by the piercing method for several hours after the start of LB medium flow containing phages (Fig. 5).

Experimental data showed that the initial concentration of unadsorbed phages in LB medium 1 h after the start

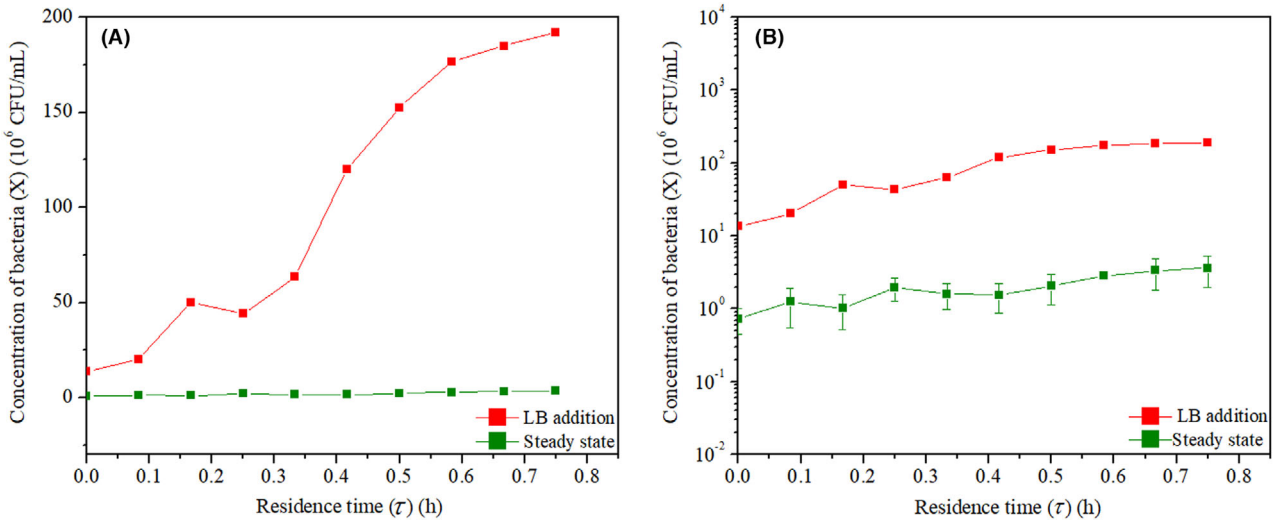

Fig. 4. Bacterial concentration in the tubular bioreactor after addition of LB medium to the biofilm. The green squares represent total bacteria steady-state concentration in the tubular bioreactor after 24 h of washing, and the red squares represent bacterial concentration after 2 h of continuous LB medium flow. The same data are shown on linear (A) and logarithmic scale (B).

of their supply was substantially lower than their loading concentration, indicating intense adsorption to the bacterial biofilm (Fig. 5A). In contrast, the increase in phage concentration along the bioreactor indicated their multiplication, demonstrating bacterial infection and lysis. This is further confirmed by the phage concentration above the loading concentration after the 2 and 3 h. Significantly, no uninfected bacteria were detected in the tubular bioreactor after only 2 h of phage supply (Fig. 5B), demonstrating their complete infection. Phages supplied together with LB medium were, therefore, able to eradicate the bacterial biofilm in the tubular bioreactor, showing plausible phage efficacy on biofilms in the presence of bacterial nutrients.

Application of phages in SM buffer

Bacterial biofilms are usually present in sub-optimal environments for bacterial growth (Ward *et al*., 1992), which might result in a substantially decreased phage multiplication or even its absence in planktonic cells, due to their low-metabolic activity (Sutherland *et al*., 2004; Golec *et al*., 2011; Nabergoj *et al*., 2018b). To examine phage effect under such conditions on biofilm, phages suspended in SM buffer were introduced, providing no bacterial nutrients. Unadsorbed phage concentration at the tubular bioreactor outlet was monitored over time (Fig. 6).

Since loading phage concentration was 9.00×10^6 PFU ml^{-1}, it can be concluded that the phages were initially adsorbed to the biofilm, while approximately 1.85 h after the start of loading (1.1 h if residence time of 0.75 h within bioreactor is considered) phage concentration similar to inlet one was reached at bioreactor outlet. Although lower initial phage concentration indicated phage adsorption, there is no clear evidence of their multiplication. Considering the difference in the average phage concentration at bioreactor outlet and inlet, one can calculate the amount of adsorbed phages according to the following equation:

$$\begin{aligned} N_P &= t \cdot F(\text{ml min}^{-1}) \times P_0 \times \left(\frac{P_{\text{t aver.}}}{P_0}\right) \\ &= (1.85-0.75)\text{h} \times 60 \text{ min h}^{-1} \times 0.2 \text{ml min}^{-1} \times \\ &\quad 9.0 \cdot 10^6 \text{PFU ml}^{-1} \times 0.9 \\ &= 1.1 \text{ h} \times 60 \text{ min h}^{-1} \times 0.2 \text{ml min}^{-1} \times \\ &\quad 9.0 \cdot 10^6 \text{ PFU ml}^{-1} \times 0.9 = 1.07 \cdot 10^8 \text{ PFU} \end{aligned} \quad (1)$$

From the number of adsorbed phages (1.07×10^8) and total concentration of bacteria, both biofilm and planktonic, MOI (multiplicity of infection) can be estimated (Equation 2):

$$\text{MOI} = \frac{P}{X} = \frac{1.07 \cdot 10^8 \text{PFU}}{3.54 \cdot 10^9 \text{CFU}} = 0.0302 \quad (2)$$

This calculation assumed that all biofilm bacteria are equally accessible to phages, which is not a realistic assumption since biofilm thickness was found to be in average of 13 {m and therefore biofilm bacteria are present in several layers. More realistically, only the upper bacterial layer is initially accessed. Considering biofilm thickness and bacteria dimensions, the upper biofilm layer consisted of approximately 2.72×10^8 CFU, resulting in an estimated MOI of 0.39. Real MOI value is

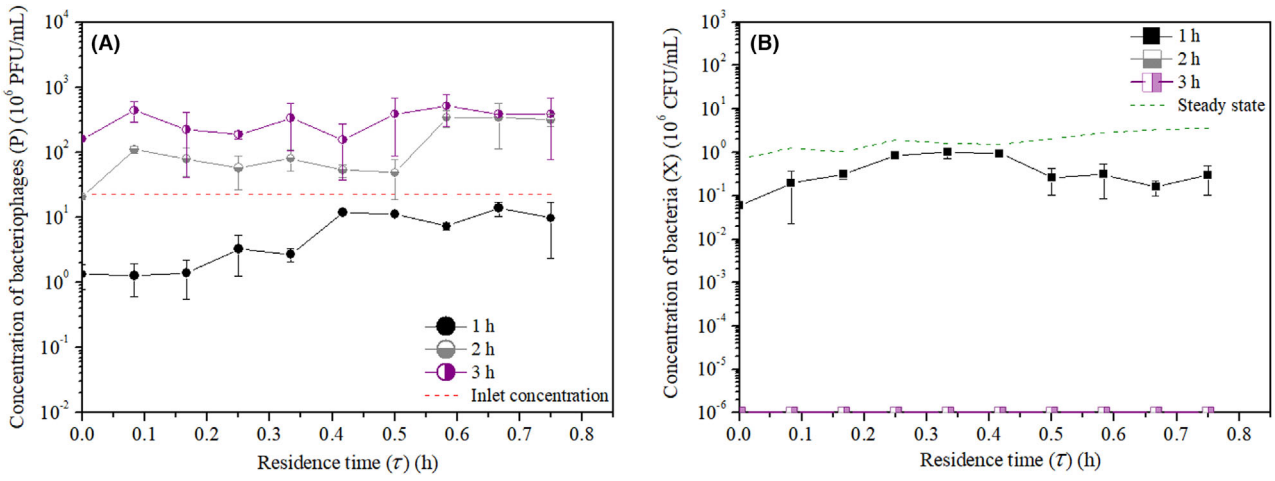

Fig. 5. Concentration of unadsorbed phages and uninfected bacteria during several hours of continuous phage supply in LB medium.
A. The red-dashed line represents supplied phage concentration (2.3×10^7 PFU ml^{-1}), while the concentration of unadsorbed phages after 1, 2, and 3 h of phage supply in LB medium are represented by circles with corresponding error bars.
B. The concentration of total bacteria in the tubular bioreactor after 24 h of washing is represented by the green dashed line, while the squares with corresponding error bars represent the uninfected bacteria along the bioreactor over time.

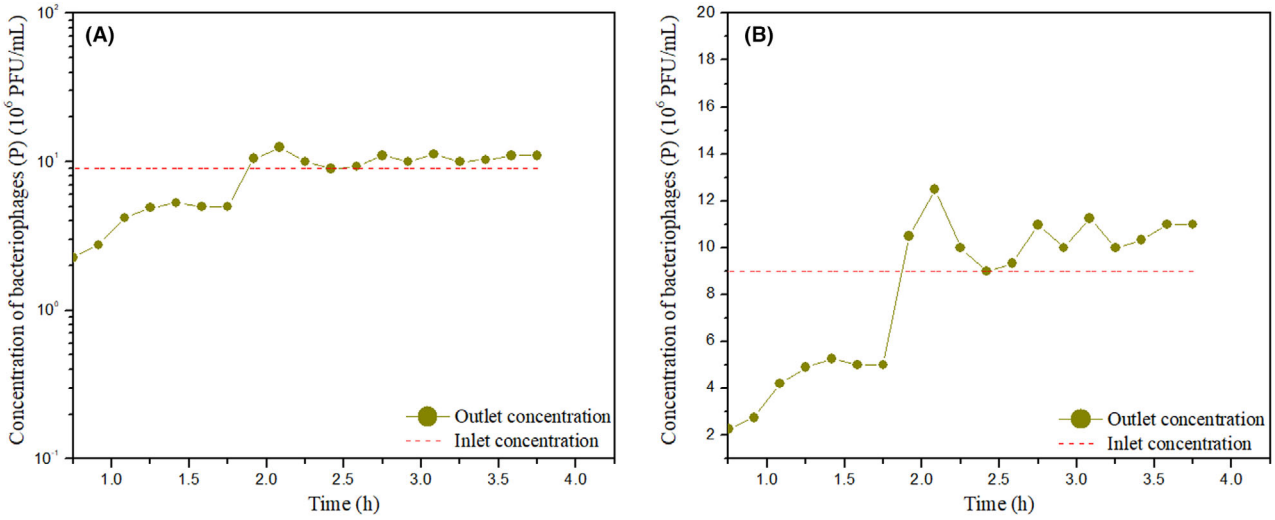

Fig. 6. Concentration of unadsorbed phages at the tubular bioreactor outlet during continuous phage supply in SM buffer. The dark yellow circles represent the concentration of unadsorbed phages at the tubular bioreactor outlet, while the red dashed line indicates supplied phage concentration (9.0×10^6 PFU ml^{-1}). The data are presented on a logarithmic scale for easier assessment of the trend (A) and on a normal scale for the calculation of adsorbed phages (B).

probably between these two values what demonstrates that only small portion of biofilm bacteria are initially infected. Therefore, it is informative to monitor the concentration of uninfected bacterial cells along the bioreactor over several hours of phage loading in SM buffer (Fig. 7A).

Compared to a decrease in bacterial biofilm concentration, when phages were supplied in LB medium, the increase in infection was much slower in this case, as uninfected bacterial cells were still present after 3 h of phage supply. Interestingly, the initial concentration of 7.25×10^5 CFU ml^{-1} dropped to 2×10^4 CFU ml^{-1} (below 3%) over this period, indicating the progressive infection of the biofilm through the layers. This might be due to phage diffusion through EPS or slow upper bacteria layer lysis, enabling phage penetration deeper into the biofilm. Discrimination between the two mechanisms is not possible solely from the measurement of phage concentration at the bioreactor outlet due to a slow dynamics of this process and consequently small concentration differences. To investigate the mechanism of infection progression, the phage supply was stopped, and the infected biofilm was washed with SM buffer for 22 h to elute all unadsorbed phages. The concentration of unadsorbed phages and uninfected bacteria after 22 h of washing along the tubular bioreactor was determined by the piercing method (Fig. 7B).

The data in Fig. 7B show the presence of uninfected bacterial cells even after 22 h of SM washing. Again, to discriminate between uninfected planktonic bacteria and uninfected biofilm bacteria, the concentration of uninfected planktonic bacteria (3.90×10^5 CFU ml^{-1}) and infected planktonic bacteria (2.50×10^5 PFU ml^{-1}) were determined from the outlet medium. The presence of both types of planktonic bacteria indicated that biofilm was still present and active. Evidently, it was not eliminated as in the case of the LB medium. Nevertheless, the increase of free phage concentration along the bioreactor (Fig. 7B) and their presence at the bioreactor outlet (determined to be 1.60×10^6 PFU ml^{-1}) indicated their weak multiplication, which can most probably be attributed to the slow lysis of the bacterial cells.

The presence of uninfected bacteria (Fig. 7B) demonstrated low phage efficiency under such conditions. As previously calculated, the bacteria in the biofilm under substrate limitation exhibited extremely slow growth of 8.95×10^{-3} h^{-1}; hence, bacteria may not possess sufficient energy for phages to propagate efficiently. Under such conditions, phage propagation in planktonic cells is significantly reduced (Golec *et al.*, 2014; Nabergoj *et al.*, 2018b), or even causes phage hibernation, in which phages infect bacteria in the stationary growth phase, inject the phage genome and initiate protein synthesis, however further phage development is stopped until new energy for bacteria is provided (Bryan *et al.*, 2016). Such impaired phage activity has also been reported for phages other than T4 infecting *Pseudomonas fluorescens* (Sillankorva *et al.*, 2004) and *Staphylococcus epidermidis* (Cerca *et al.*, 2007). Interestingly, it was recently discovered that after prolonged exposure of a stationary culture of *Staphylococcus epidermidis* to bacteriophage SEP1, bacterial cells were efficiently lysed despite reduced phage multiplication (Melo *et al.*, 2018). This work reveals the complexity

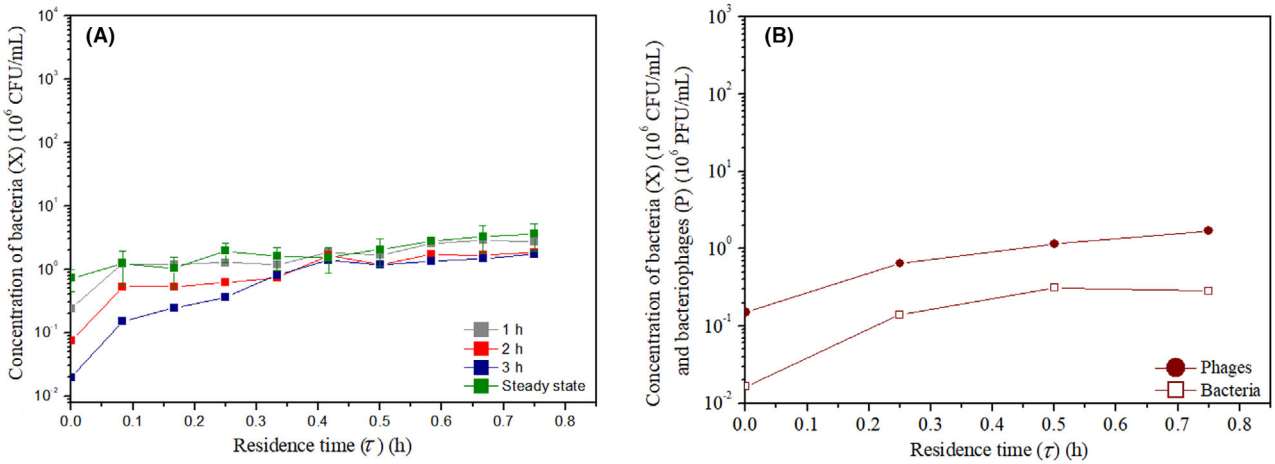

Fig. 7. Concentration of uninfected bacteria after several hours of continuous phage flow in SM buffer (A) and phage and bacteria concentration in the tubular bioreactor after 22 h of washing with SM buffer (B).
A. The grey, red, and blue squares represent a concentration of uninfected bacteria over time. For comparison, the green dashed line shows the initial total bacterial steady-state concentration.
B. The concentration of free, unadsorbed phages in the tubular bioreactor is shown as PFU ml^{-1} by circles, whereas squares show the corresponding concentration of unadsorbed bacteria in the tubular bioreactor as CFU ml^{-1}.

of interactions between bacteria and phages and shows that experiments should be performed on a particular system.

Therefore, further experiments with phage-infected and washed biofilm were conducted to investigate whether phages that may be present in the biofilm can be effective when more favourable conditions for bacterial growth occur. A constant flow of LB medium without phages was supplied to the tubular bioreactor containing the infected biofilm and, since bacterial biofilm susceptibility to fresh nutrients has already been demonstrated by an increased specific growth rate (Fig. 4), the addition of the LB medium might also result in significantly faster phage propagation. Phage and bacterial concentrations along the bioreactor and at the bioreactor outlet were monitored after the fresh substrate supply (Fig. 8).

By monitoring the concentration of uninfected bacteria along the tubular bioreactor after the start of the continuous LB medium supply, one can see that the number of bacteria was rapidly decreasing over time (Fig. 8A) to undetectable levels after only 2 h. An increase in phage concentration over time can be seen, both along the bioreactor (Fig. 8B) and at the bioreactor outlet (Fig. 8C), confirming bacterial lysis and the release of new unadsorbed phages capable of further infection to finally eradicate bacterial biofilm. This demonstrated how phage propagation is deeply connected to bacterial physiological state and confirmed potential of phages that remained inside the biofilm (either hibernating or just physically entrapped) to lyse both planktonic and biofilm bacteria when an energy source is provided.

The development of an experimental set-up consisting of connected continuously operating mixing and tubular bioreactors enabled the reproducible formation of a bacterial biofilm and, in combination with the piercing method, the monitoring of bacterial and phage profiles along the tubular bioreactor. Proof of principle was demonstrated on model microorganisms, since a stable *E. coli* biofilm was formed within 24 h after bacterial supply and subsequent buffer washing. Results confirmed that phage efficacy is highly depended on the physiological state of the biofilm bacteria, and reduced phage multiplication was observed under bacteria starvation conditions, similar as for planktonic bacteria. Due to its simplicity and versatility, the presented experimental set-up can be used as a platform approach to study bacterial biofilm formation, generation of planktonic cells and the effect of phage treatment, under different growth conditions.

Experimental procedures

Bacteria, phage, and media

The bacteria strain *Escherichia coli* K-12 MG1655 (DSM 18039) from the Leibniz Institute DSMZ Germany was used for biofilm formation and titration of the T4 lytic phage (DSM 4505). Bacteria for phage titer determination and initial inoculation of the chemostat were prepared in laboratory flasks in Lysogeny Broth (LB) (LLG Labware, Meckenheim, Germany) and incubated overnight at 37°C (Sambrook and Russel, 2001). An LB medium was used to grow the continuous bacterial culture in the chemostat and biofilm formation. For biofilm

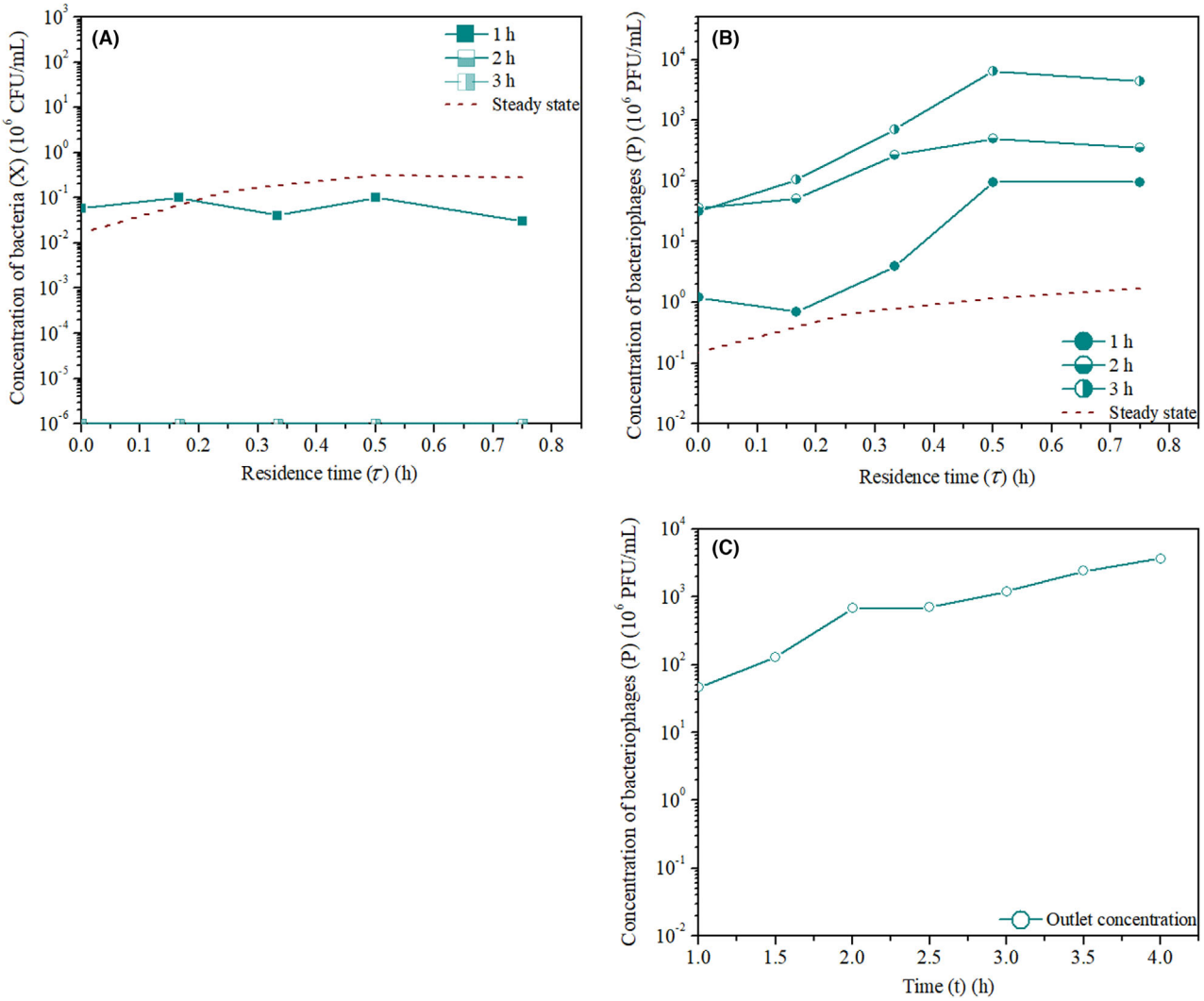

Fig. 8. Concentration of unadsorbed phages and uninfected bacteria after the introduction of LB medium flow to infected and washed biofilm. The concentration of uninfected bacteria along the bioreactor after several hours of LB flow is represented by cyan squares and, for comparison, the concentration of bacteria after 22 h of SM buffer washing (Fig. 7B) is represented by the brown dashed line (A). Unadsorbed phage concentrations over time along the bioreactor are represented by cyan circles (B), with the phage concentration after 22 h of SM buffer washing (Fig. 7B) represented as the brown dashed line, while the phage concentration at the outlet after LB medium addition is represented by blank circles (C).

washing and determination of phage titer, an SM buffer (1 g gelatin (Sigma-Aldrich, St. Louis, MO, USA), 5.8 g NaCl (Merck KGaA, Darmstadt, Germany), 2 g $MgSO_4 \cdot 7H_2O$ (Merck KGaA, Darmstadt, Germany), 50 ml 1 M Tris–HCl (pH 7.5) (Fisher Scientific F, Loughborough, UK), deionized water to 1 l) was used.

Bacteria and phage enumeration

Enumeration of *E. coli* bacteria was done using an agar layer method, and the number of bacteria was expressed as colony-forming units (CFU), while phage enumeration was done using the standard double agar overlay plaque assay, and their concentration was determined as plaque-forming units (PFU) (Clokie and Kropinski, 2009) by filtering the sample through a sterile 0.22 μm syringe filter (LLG Labware, Meckenheim, Germany). All assays were performed in triplicate and average value was calculated.

Continuous cultivation of free-floating bacteria

Escherichia coli bacteria were cultivated at 37°C in a chemostat system consisting of a glass bioreactor with 25 ml working volume stirred with a magnetic stirrer at 350 rpm, as described by Nabergoj *et al.* (2018a). The LB medium saturated with prefiltered air was continuously supplied to the growing bacteria in the bioreactor at a flow rate of

0.1 ml min^{-1}, corresponding to a dilution rate of 0.24 h^{-1}. The concentration of bacteria was monitored by online measurement of optical density at a wavelength of 600 nm. After 10 bacterial generations of continuous growth, a steady state was reached, and the concentration of bacteria in the bioreactor was determined.

Biofilm experiments

To study the interaction of bacterial biofilms with phages, a series of experiments were performed (Fig. 1C) using continuously operating system at 37°C (Fig. 1A). A constant flow rate of 0.2 ml min^{-1} through a tubular bioreactor (a silicone tube of 0.46 m length and 5 mm inner diameter) enabled a stable flow regime in the bioreactor, while changes in the composition of the inlet flow enabled studying the effect of different conditions. The residence time within the tubular bioreactor was 0.75 h.

Biofilm formation. The LB medium from the chemostat containing approximately 9.0×10^7 bacterial cells per mL was continuously combined with a stream of SM buffer and fed into the tubular bioreactor for 2 h to allow bacterial cell adhesion. This was followed by extensive washing with the SM buffer for 24 h to remove unadsorbed bacterial cells and to reduce the metabolic activity of the attached cells due to a substrate limitation. This procedure resulted in the formation of a reproducible biofilm that was used for all further experiments. Three independent experiments were performed in duplicate and average value and standard deviation were calculated.

The bacterial cell concentration inside the tubular bioreactor during biofilm formation was monitored via a piercing method, sampling the volume of 50 μl with the use of sterile syringe needles (Chirana T. injecta) of 1 ml working volume (see Results and discussion section for a detailed description of the method) after 1 h of bacteria supply and after 1, 2, 3, 22, and 24 h of SM buffer wash on different positions along tubular bioreactor. The concentration of only planktonic bacteria was determined in the medium exiting the tubular bioreactor.

Application of LB medium to formed biofilm. To assess the viability of the formed biofilm, only the LB medium was introduced into the tubular bioreactor. Bacterial concentration was monitored along the tubular bioreactor after 2 h of continuous LB medium supply using the piercing method. Two independent experiments were performed in duplicate and an average value was calculated.

Application of phages in LB medium to formed biofilm. Phage concentration of 1.5×10^7 PFU ml^{-1} in LB medium was continuously supplied to the biofilm. After 1, 2, and 3 h of phage supply, the concentration of unadsorbed phages and uninfected bacteria inside the tubular bioreactor was determined by the piercing method. Unadsorbed phages were determined by filtering the sample through a sterile 0.22 μm syringe filter. Two independent experiments were performed in duplicate and average value was calculated.

Application of phages in SM buffer to the formed biofilm. Phage concentration of 9×10^6 PFU ml^{-1} in SM buffer was continuously supplied to the biofilm for 4 h. Due to specificity of experimental set-up, detailed discussion about MOI estimation is presented in section Application of phages in SM buffer. After 1, 2, and 3 h of phage supply, the concentration of unadsorbed phages and uninfected bacteria inside the tubular bioreactor was determined by the piercing method. Samples were also collected at the tubular bioreactor outlet to determine uninfected and infected planktonic bacteria and unadsorbed phages, with infected planktonic bacteria determined by a double agar overlay plaque assay without filtering the sample.

The bacterial biofilm infected by phages in the SM buffer was subsequently washed with the SM buffer without phages for 16 h to remove unadsorbed phages. The concentrations of uninfected planktonic bacteria, infected planktonic bacteria, and unadsorbed phages were determined from the bioreactor outlet medium after washing was completed. After that, the SM buffer was replaced with LB medium to provide nutrients to the bacteria in the bioreactor. The concentration of uninfected planktonic bacteria and unadsorbed phages was monitored every 15 min for 4 h in the bioreactor outlet medium. The concentration of unadsorbed phages and uninfected bacteria along the tubular bioreactor was monitored after 1, 2, and 3 h by the piercing method. Three independent experiments were performed in duplicate and average value was calculated.

Acknowledgements

The financial support is gratefully acknowledged from the Slovenian Research Agency (ARRS) through programme P1-0153 and project J7-2603 as well as from project IMBI co-financed by European Regional Development Fund, Interreg V-A Italy-Slovenia programme 2014-2020.

Conflict of interest

There are no conflicts of interest with the authors of this work.

Authors contributions

AL and AP contributed to the design of the research. AL and EB carried out the experiments and measurements. AL and AP analysed the results and prepared the manuscript.

Data availability statement

The data that supports the findings of this study are available in the supplementary material of this article.

References

Abedon, S.T. (2011) *Bacteriophages and Biofilms: Ecology, Phage Therapy, Plaques*. New York: Nova Science Publishers.

Abedon, S.T. (2015) Ecology of anti-biofilm agents II: bacteriophage exploitation and biocontrol of biofilm bacteria. *Pharmaceuticals* **8:** 559–589.

Abedon, S.T., Herschler, T.D., and Stopar, D. (2001) Bacteriophage latent-period evolution as a response to resource availability. *Appl Environ Microbiol* **67:** 4233–4241.

Ackermann, H.W., and Prangishvili, D. (2012) Prokaryote viruses studied by electron microscopy. *Arch Virol* **157:** 1843–1849.

Alves, D.R., Perez-Esteban, P., Kot, W., Bean, J.E., Arnot, T., Hansen, L.H. *et al*. (2016) A novel bacteriophage cocktail reduces and disperses Pseudomonas aeruginosa biofilms under static and flow conditions. *J Microbial Biotechnol* **9:** 61–74.

Azeredo, J., García, P., and Drulis-Kawa, Z. (2021) Targeting biofilms using phages and their enzymes. *Curr Opin Biotechnol* **68:** 251–261.

Beloin, C., and Ghigo, J.M. (2005) Finding gene-expression patterns in bacterial biofilms. *Trends Microbiol* **13:** 16–19.

Bjarnsholt, T. (2013) The role of bacterial biofilms in chronic infections. *APMIS Suppl* **121:** 1–51.

Bryan, D., El-Shibiny, A., Hobbs, Z., Porter, J., and Kutter, E.M. (2016) Bacteriophage T4 infection of stationary phase *E. coli*: life after log from a phage perspective. *Front Microbiol* **7:** 1–12.

Burmølle, M., Webb, J.S., Rao, D., Hansen, L.H., Sørensen, S.J., and Kjelleberg, S. (2006) Enhanced biofilm formation and increased resistance to antimicrobial agents and bacterial invasion are caused by synergistic interactions in multispecies biofilms. *Appl Environ Microbiol* **72:** 3916–3923.

Cenens, W., Makumi, A., Tesfazgi Mebrhatu, M., Lavigne, R., and Aertsen, A. (2013) Phage-host interactions during pseudolysogeny. *Bacteriophage* **3:** 1–4.

Cerca, N., Oliveira, R., and Azeredo, J. (2007) Susceptibility of Staphylococcus epidermidis planktonic cells and biofilms to the lytic action of staphylococcus bacteriophage K. *Lett Appl Microbiol* **45:** 313–317.

Clokie, M.R.J., and Kropinski, A.M. (2009) *Bacteriophages: Methods and Protocols, Volume 1: Isolation*. New York: Humana Press, a part of Springer Science Business Media.

Corbin, B.D., McLean, R.J.C., and Aron, G.M. (2001) Bacteriophage T4 multiplication in a glucose-limited *Escherichia coli* biofilm. *Can J Microbiol* **47:** 680–684.

Costerton, J.W., Stewart, P.S., and Greenberg, E.P. (1999) Bacterial biofilms: a common cause of persistent infections. *Science* **284:** 1318–1322.

Costerton, W., Veeh, R., Shirtliff, M., Pasmore, M., Post, C., and Ehrlich, G. (2003) The application of biofilm science to the study and control of chronic bacterial infections. *J Clin Invest* **112:** 1466–1477.

Davies, D. (2003) Understanding biofilm resistance to antibacterial agents. *Nat Rev Drug Discov* **2:** 114–122.

Davies, D.G., Chakrabarty, A.M., and Geesey, G.G. (1993) Exopolysaccharide production in biofilms: substratum activation of alginate gene expression by Pseudomonas aeruginosa. *Appl Environ Microbiol* **59:** 1181–1186.

Davies, D.G., and Geesey, G.G. (1995) Regulation of the alginate biosynthesis gene algC in Pseudomonas aeruginosa during biofilm development in continuous culture. *Appl Environ Microbiol* **61:** 860–867.

De la Fuente-Núñez, C., Reffuveille, F., Fernández, L., and Hancock, R.E.W. (2013) Bacterial biofilm development as a multicellular adaptation: antibiotic resistance and new therapeutic strategies. *Curr Opin Microbiol* **16:** 580–589.

Dhayakaran, R., and Neethirajan, S. (2017) Microscopic methods in biofilm research. In *Biofilms: Emerging Concepts and Trends*. Murthy, S. (ed). New Delhi, India: Narosa Publishers, pp. 208.

Donlan, R.M. (2001) Biofilms and device-associated infections. *Emerg Infect Dis* **7:** 277–281.

Donlan, R.M. (2002) Biofilms: microbial life on surfaces. *Emerg Infect Dis* **8:** 881–890.

Doolittle, M.M., Cooney, J.J., and Caldwell, D.E. (1995) Lytic infection of Escherichia coli biofilms by bacteriophage T4. *Can J Microbiol* **41:** 12–18.

Flemming, H.C., Neu, T.R., and Wozniak, D.J. (2007) The EPS matrix: The "House of Biofilm Cells.". *J Bacteriol* **189:** 7945–7947.

Flemming, H.C., and Wingender, J. (2010) The biofilm matrix. *Nat Rev Microbiol* **8:** 623–633.

Forti, F., Roach, D.R., Cafora, M., Pasini, M.E., Horner, D.S., Fiscarelli, E.V. *et al*. (2018) Design of a broad-range bacteriophage cocktail that reduces pseudomonas aeruginosa biofilms and treats acute infections in two animal models. *Antimicrob Agents Chemother* **62:** 6.

Golec, P., Karczewska-Golec, J., Loś, M., and Wegrzyn, G. (2014) Bacteriophage T4 can produce progeny virions in extremely slowly growing Escherichia coli host: comparison of a mathematical model with the experimental data. *FEMS Microbiol Lett* **351:** 156–161.

Golec, P., Wiczk, A., Łoś, J.M., Konopa, G., Wegrzyn, G., and Łoś, M. (2011) Persistence of bacteriophage T4 in a starved Escherichia coli culture: evidence for the presence of phage subpopulations. *J Gen Virol* **92:** 997–1003.

Guzmán-Soto, I., McTiernan, C., Gonzalez, M., Ross, A., Gupta, K., Suuronen, E.J. *et al*. (2021) Mimicking Biofilm Formation and Development: Recent Progress in in vitro and in vivo Biofilm Models. *iScience* **24:** 1–41.

Hadas, H., Einav, M., and Zaritsky, A. (1994) Development depends on the physiology. *J Bacteriol* **143:** 179–185.

Hadas, H., Einav, M., and Zaritsky, A. (1997) Bacteriophage T4 development depends on the physiology of its host *E. coli*. *Microbiology* **143:** 179–185.

Hall-Stoodley, L., Costerton, J.W., and Stoodley, P. (2004) Bacterial biofilms: from the natural environment to infectious diseases. *Nat Rev Microbiol* **2:** 95–108.

Hansen, M.F., Svenningsen, S.L., Røder, H.L., Middelboe, M., and Burmølle, M. (2019) Big impact of the tiny: bacteriophage – bacteria interactions in bio fi lms. *Trends Microbiol* **27:** 739–752.

Hughes, K.A., Sutherland, I.W., Clark, J., and Jones, M.V. (1998a) Bacteriophage and associated polysaccharide depolymerases - novel tools for study of bacterial biofilms. *J Appl Microbiol* **85:** 583–590.

Hughes, K.A., Sutherland, I.W., and Jones, M.V. (1998b) Biofilm susceptibility to bacteriophage attack: the role of phage-borne polysaccharide depolymerase. *Microbiology* **144:** 3039–3047.

Jamal, M., Ahmad, W., Andleeb, S., Jalil, F., Imran, M., Nawaz, M.A. *et al*. (2018) Bacterial biofilm and associated infections. *J Chinese Med Assoc* **81:** 7–11.

Keleştemur, S., Avci, E., and Çulha, M. (2018) Raman and surface-enhanced Raman scattering for biofilm characterization. *Chemosensors* **6:** 1–15.

Koseoglu, H., Aslan, G., Esen, N., Sen, B.H., and Coban, H. (2006) Ultrastructural stages of biofilm development of Escherichia coli on urethral catheters and effects of antibiotics on biofilm formation. *Urology* **68:** 942–946.

Lambe, D.W., Ferguson, K.P., Mayberry-Carson, K.J., Tober-Meyer, B., and Costerton, J.W. (1991) Foreign-body-associated experimental osteomyelitis induced with Bacteroides fragilis and Staphylococcus epidermidis in rabbits. *Clin Orthop Relat Res* **266:** 285–294.

Lewis, K. (2001) Riddle of biofilm resistance. *Antimicrob Agents Chemother* **45:** 999–1007.

Łoś, M., and Wegrzyn, G. (2012) Pseudolysogeny. In *Advances in Virus Research*. Szybalski, W.T., and Łobocka, M. (eds). Cambridge: Academic Press, pp. 339–349.

Mah, T.F.C., and O'Toole, G.A. (2001) Mechanisms of biofilm resistance to antimicrobial agents. *Trends Microbiol* **9:** 34–39.

Marrie, T.J., Nelligan, J., and Costerton, J.W. (1982) A scanning and transmission electron microscopic study of human nodular goitre. *Circulation* **66:** 65–76.

McLean, R.J.C., Corbin, B.D., Balzer, G.J., and Aron, G.M. (2001) Phenotype characterization of genetically defined microorganisms and growth of bacteriophage in biofilms. *Methods Enzymol* **336:** 163–174.

Melo, L.D.R., França, A., Brandão, A., Sillankorva, S., Cerca, N., and Azeredo, J. (2018) Assessment of Sep1-virus interaction with stationary cultures by transcriptional and flow cytometry studies. *FEMS Microbiol Ecol* **94:** 1–8.

Nabergoj, D., Kuzmić, N., Drakslar, B., and Podgornik, A. (2018a) Effect of dilution rate on productivity of continuous bacteriophage production in cellstat. *Appl Microbiol Biotechnol* **102:** 3649–3661.

Nabergoj, D., Modic, P., and Podgornik, A. (2018b) Effect of bacterial growth rate on bacteriophage population growth rate. *Microbiol Open* **7:** 1–10.

O'Toole, G.A., and Kolter, R. (1998) Flagellar and twitching motility are necessary for Pseudomonas aeruginosa biofilm development. *Mol Microbiol* **30:** 295–304.

Read, R.R., Eberwein, P., Dasgupta, M.K., Grant, S.K., Lam, K., Nickel, J.C., and Costerton, J.W. (1989) Peritonitis in peritoneal dialysis: bacterial colonization by biofilm spread along the catheter surface. *Kidney Int* **35:** 614–621.

Reshes, G., Vanounou, S., Fishov, I., and Feingold, M. (2008) Cell shape dynamics in Escherichia coli. *Biophys J* **94:** 251–264.

Riley, M. (1999) Correlates of Smallest Sizes for Microorganisms. In *Size Limits of Very Small Microorganisms: Proceedings of a Workshop*. Washington, DC: National Academies Press, pp. 21–25.

Sambrook, J.F., and Russel, D.W. (2001) *Molecular Cloning: A Laboratory Manual*. 3rd ed. New York: Cold Spring Harbor Laboratory Press.

Sauer, K., Camper, A.K., Ehrlich, G.D., Costerton, J.W., and Davies, D.G. (2002) Pseudomonas aeruginosa displays multiple phenotypes during development as a biofilm. *J Bacteriol* **184:** 1140–1154.

Sharma, D., Misba, L., and Kan, A.U. (2019) Antibiotics versus biofilm: an emerging battleground in microbial communitiesIEnhanced Reader. *Antimicrob Resist Infect Control* **3:** 1–10.

Sharma, G., Sharma, S., Sharma, P., Chandola, D., Dang, S., Gupta, S., and Gabrani, R. (2016) *Escherichia coli* biofilm: development and therapeutic strategies. *J Appl Microbiol* **121:** 309–319.

Sillankorva, S., Oliveira, R., Vieira, M.J., Sutherland, I., and Azeredo, J. (2004) Pseudomonas fluorescens infection by bacteriophage Φs1: the influence of temperature, host growth phase and media. *FEMS Microbiol Lett* **241:** 13–20.

Simmons, M., Drescher, K., Nadell, C.D., and Bucci, V. (2018) Phage mobility is a core determinant of phage-bacteria coexistence in biofilms. *ISME J* **12:** 532–543.

Sønderholm, M., Bjarnsholt, T., Alhede, M., Kolpen, M., Jensen, P., Kühl, M., and Kragh, K.N. (2017) The consequences of being in an infectious biofilm: microenvironmental conditions governing antibiotic tolerance. *Int J Mol Sci* **18:** 15–17.

Sternberg, C., Christensen, B.B., Johansen, T., Nielsen, A.T., Andersen, J.B., Givskov, M., and Molin, S. (1999) Distribution of bacterial growth activity in flow-chamber biofilms. *Appl Environ Microbiol* **65:** 4108–4117.

Stewart, P.S. (2015) Antimicrobial tolerance in biofilms examples of reduced biofilm susceptibility. *Microbiol Spectr* **3:** 1–30.

Stickler, D.J. (1996) Bacterial biofilms and the encrustation of urethral catheters. *Biofouling* **9:** 293–305.

Stoodley, P., Dodds, I., Boyle, J.D., and Lappin-Scott, H.M. (1999) Influence of hydrodynamics and nutrients on biofilm structure. *J Appl Microbiol Symp Suppl* **85:** 19–28.

Stoodley, P., Wilson, S., Hall-Stoodley, L., Boyle, J.D., Lappin-Scott, H.M., and Costerton, J.W. (2001) Growth

and detachment of cell clusters from mature mixed-species biofilms. *Appl Environ Microbiol* **67:** 5608–5613.

Su, P.-T., Liao, C.-T., Roan, J.-R., Wang, S.-H., Chiou, A., and Syu, W. (2012) Bacterial colony from two-dimensional division to three-dimensional development. *PLoS One* **7:** 1–10.

Sutherland, I.W., Hughes, K.A., Skillman, L.C., and Tait, K. (2004) The interaction of phage and biofilms. *FEMS Microbiol Lett* **232:** 1–6.

Svensson Malchau, K., Tillander, J., Zaborowska, M., Hoffman, M., Lasa, I., Thomsen, P. *et al.* (2021) Biofilm properties in relation to treatment outcome in patients with first-time periprosthetic hip or knee joint infection. *J Orthop Transl* **30:** 31–40.

Tolker-Nielsen, T., Brinch, U.C., Ragas, P.C., Andersen, J.B., Jacobsen, C.S., and Molin, S. (2000) Development and dynamics of Pseudomonas sp. biofilms. *J Bacteriol* **182:** 6482–6489.

Tuson, H.H., and Weibel, D.B. (2014) Bacteria-surface interactions. *Soft Matter* **9:** 4368–4380.

Vu, B., Chen, M., Crawford, R.J., and Ivanova, E.P. (2009) Bacterial extracellular polysaccharides involved in biofilm formation. *Molecules* **14:** 2535–2554.

Ward, K.H., Olson, M.E., Lam, K., and Costerton, J.W. (1992) Mechanism of persistent infection associated with peritoneal implants. *J Med Microbiol* **36:** 406–413.

Whiteley, M., Bangera, M.G., Bumgarner, R.E., Parsek, M.R., Teitzel, G.M., Lory, S., and Greenberg, E.P. (2001) Gene expression in Pseudomonas aeruginosa biofilms. *Nature* **413:** 860–864.

Wilks, S.A., Koerfer, V.V., Prieto, J.A., Fader, M., and Keevil, C.W. (2021) Biofilm development on urinary catheters promotes the appearance of viable but nonculturable bacteria. *MBio* **12:** 2.

Zhang, X., Bishop, P.L., and Kupferle, M.J. (1998) Measurement of polysaccharides and proteins in biofilm extracellular polymers. *Water Sci Technol* **37:** 345–348.

Supporting information

Additional supporting information may be found online in the Supporting Information section at the end of the article.

Fig. S1. Concentration of *E. coli* in the tubular bioreactor after 1 h of continuous bacterial feeding. A stream consisting of SM buffer and bacteria in LB medium was supplied at 0.2 ml min^{-1}. Bacteria were sampled by the piercing method at different positions of the tubular bioreactor, corresponding to residence times (τ) from $\tau = 0$ h (at the beginning of the bioreactor) to $\tau = 0.75$ h (end of the bioreactor). Bacterial concentration is presented with error bars as CFU ml^{-1}.

Fig. S2. Microscopic images of bacterial biofilm after 24 h of continuous SM buffer flow through the tubular bioreactor under transmission light at residence times (A) 15 min, (B) 30 min and (C) 45 min.

